

K.H. Horstmann  
A. Quast G. Redeker  
Deutsche Forschungs- und Versuchsanstalt für Luft- und  
Raumfahrt e.V. (DFVLR), Institut für Entwurfsaerodynamik  
D-3300 Braunschweig, Fed. Rep. Germany

Abstract

For the design of laminar airfoils reliable transition prediction criterions are indispensable. By means of the linear stability theory of laminar boundary layers the transition prediction procedure can be based on a sophisticated background. This paper describes carefully planned and executed experiments in free flight and in windtunnel for the determination of limiting N-values of Tollmien-Schlichting waves to serve as transition criterion. The results show that the limiting N-values are nearly independent from Reynolds number and are in the windtunnel of the same order of magnitude as in free flight, demonstrating the excellent flow quality of the windtunnel used.

Notations

x	m	streamwise coordinate of wing section
l	m	chord length of reference wing section
x/l	-	dimensionless coordinate in streamwise direction
$A_0$		initial amplitude of waves in the laminar boundary layer at the instability point
A		amplitude of amplified Tollmien-Schlichting waves in the laminar boundary layer
f	$s^{-1}$	frequency of Tollmien-Schlichting waves
N		amplification exponent or N-factor after linear stability theory ( $N = \ln(A/A_0)$ ) obtained after integration of local amplification rates
Re		Reynolds number based on reference chord
$Re_T$		Reynolds number based on length of laminar boundary layer
$c_p$		static pressure coefficient on wing contour

1. Introduction

The crucial point in the design process of laminar airfoils is the prediction of the transition location. It is only possible to estimate the performance of such airfoils, e.g. the drag polars with the

laminar drag bucket, if reliable transition criterions can be used. Although the development of CFD has reached a high standard and high speed computers are available the pure calculation of the transition process and especially the transition location is up to now not possible.

Therefore all transition prediction methods are more or less empirical and need some experimental input. For this reason it becomes obvious that various transition criterions show a broad band of scattering depending on the kind and the quality of the data from which they have been derived, e.g. experiments from different windtunnels or data from flight tests. On the other hand transition criterions can only be applied reasonably in that data region which has formed the basis of the criterion.

The well-known empirical criterions of Granville [1], Michel [2] or others are mostly based on windtunnel data taken at low Reynolds numbers and therefore it cannot be recommended to use these criterions for an airfoil design for higher Reynolds numbers in the region of  $Re = 10 \cdot 10^6$ . For this reason it was decided in the Institute of Design Aerodynamics of DFVLR to carry out transition investigations with the following objectives:

- Perform transition investigations on a suitable wing in flight and in windtunnel by carefully planned and executed measurements.
- Derive a reliable transition prediction procedure from these investigations in the Reynolds number range up to  $10 \cdot 10^6$ .
- Derive a reasonable correlation procedure between flight and windtunnel data.

2. Transition prediction with the N-factor method

A more reliable and sophisticated procedure to determine the transition location compared to simple empirical laws is the application of the  $e^N$ - or N-factor method [3,4,5,6]. Based on the stability theory of laminar boundary layers [7], this method allows the calculation of amplification rates of disturbances of various wave lengths and frequencies, the so-called Tollmien-Schlichting waves, (Fig. 1). From these amplification rates the amplification ratio and the amplification exponent N can be determined. If it

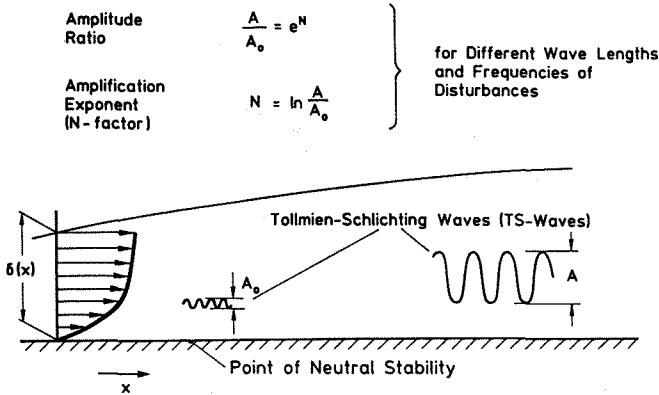


Fig. 1 Instability of Laminar Boundary Layers

is assumed that a disturbance has a basic amplitude  $A_0$  when it starts amplifying first, then the amplification ratio  $A/A_0$  at any point can be calculated by integrating the amplification rates up to this point. The amplification ratio can be expressed by an exponential function  $e^N$  where  $N$  is the amplification exponent or the so-called N-factor. It describes the growth of disturbances and must be evaluated for various wave lengths and frequencies so that  $N$  becomes a maximum value.

The use of this procedure for transition prediction can be described as follows: From carefully performed experiments the maximum calculated N-factor at the experimentally determined transition location will be evaluated and will serve as a limiting N-value in a transition prediction process [8]. For this reason adequate experiments should at least comprise:

- Pressure distribution on wing surface.
- Transition location on wing surface for the same flow conditions.

The first information is needed to perform a boundary layer calculation followed by a stability analysis with N-factor integration, while the second information is necessary for the determination of the limiting N-value.

### 3. Test aircraft LFU-205

Flight and windtunnel tests were carried out with the LFU-205 aircraft (Fig. 2), built by Leichtflugtechnik-Union GmbH, F.R.G.. The LFU-205 is a four-seat experimental prototype light aircraft. Its airframe is built completely out of glass-fibre reinforced plastic. The LFU-205 is the only prototype and made its first flight in 1968 with the main objectives of studying the effect of weight reduction by the use of light weight plastics.

The main dimensions are given in Fig. 2. The maximum cruising speed is

330 km/h leading to a Reynolds number of  $Re \approx 10 \cdot 10^6$  based on the aerodynamic mean chord. The wing is equipped with an Eppeler-airfoil E502 which is not well suited for the purpose of the planned investigations, as shown in Fig. 3. The pressure distribution on the upper surface, calculated with the Eppeler-Somers code [9], is of such type that transition possibly will take place through a small laminar separation bubble. This is confirmed by a stability analysis with the SALLY-code [10], shown below the pressure distribution. For different frequencies of TS-waves the N-factor development along the airfoil chord is plotted. It leads to an exponential rise in the region of the slight adverse pressure gradient. This behaviour at low N-factors indicates the existence of a laminar separation bubble and it is not suited to determine limiting N-values, as described before. When trying to cut the N-factor curves with steep gradients with the line  $x/l = \text{const.}$  at the measured transition location, small changes in  $\Delta x$  will result in large changes of the limiting N-values (comp. [6]).

Therefore a new wing section on the basis of E502 airfoil has been designed to overcome the described difficulties. Fig. 4 shows the pressure distribution of the new design for the same flight conditions as before. It is indicated that the upper surface of the new design shows a slight pressure rise from 20% to 70% of the airfoil chord leading to an unstable

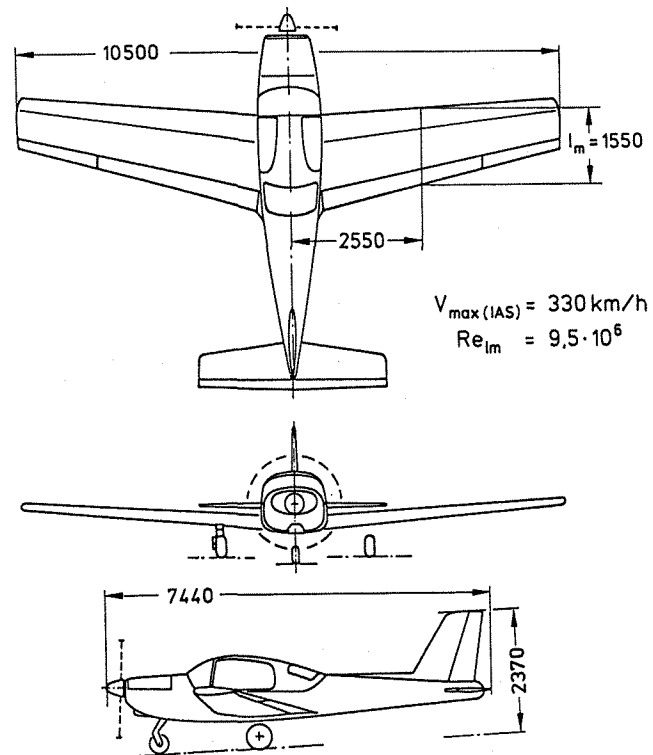


Fig. 2 Flight Test Aircraft LFU-205 (Dimensions in mm)

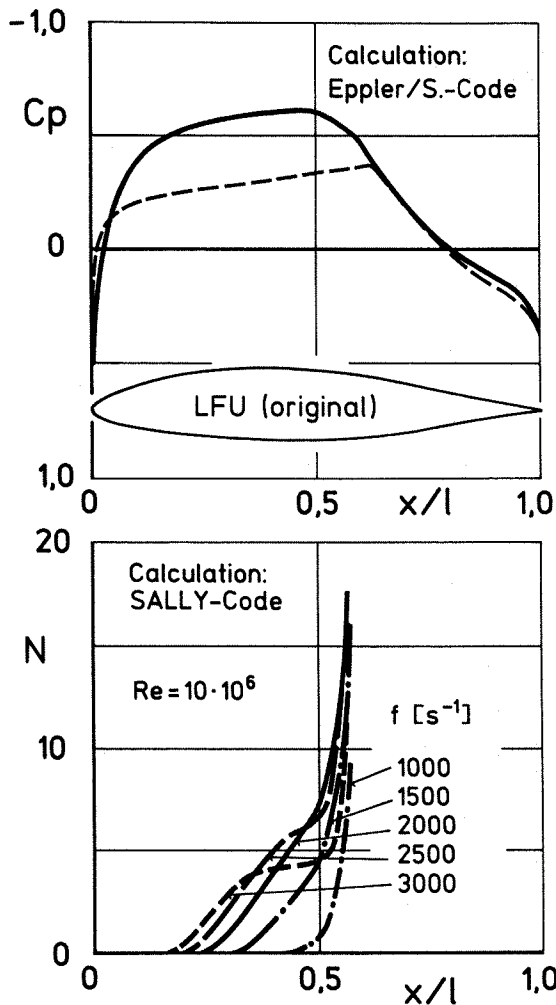


Fig. 3 Pressure Distribution and Growth of N-Factor of TS-Waves on LFU-205 Wing

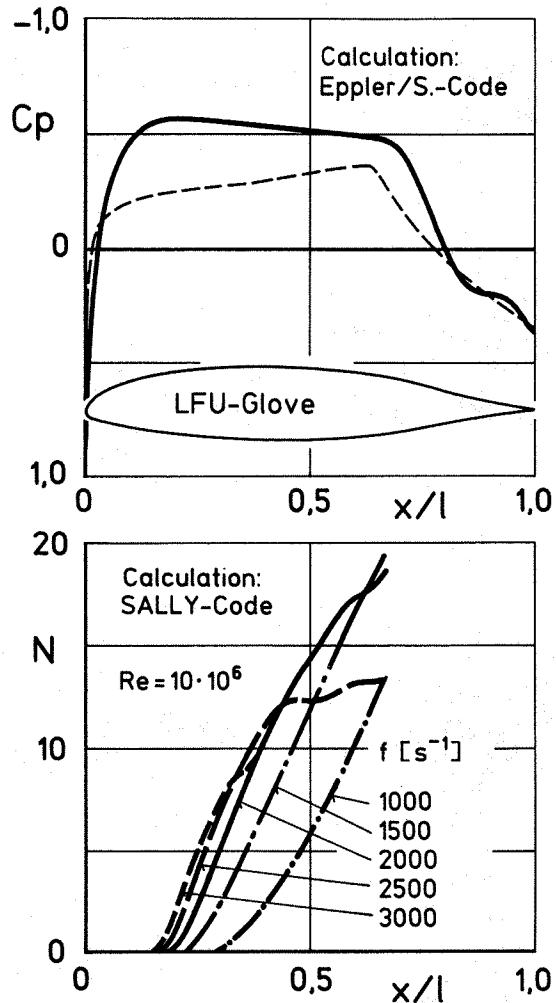


Fig. 4 Pressure Distribution and Growth of N-Factor of TS-Waves on LFU-205 Glove

laminar boundary layer, which should run into transition before laminar separation will occur in the rear part of the airfoil.

The development of the N-factors for TS-waves of various frequencies shows the desired behaviour: a nearly linear rise with increasing chord length. With this type of behaviour it is easy to determine limiting N-values at the transition location because a clear cut between N-factor curve and  $x/l = \text{const.}$  can be made.

Fig. 5 shows a comparison of the new wing section wrapped around the original LFU-205 one. The main differences occur on the upper surface near the airfoil leading edge and in the region from 50% to 70% of airfoil chord, whereas the contour of the lower surface remains nearly unchanged. There is a minimum space of 5 mm between new contour and original one allowing the installation of the tubing for the pressure orifices. There are 74 pressure orifices distributed around the airfoil contour with 0.3 mm  $\phi$  with a very dense distribu-

tion in the estimated transition region on the upper surface.

With this new wing section a glove on the right wing has been constructed shown in Fig. 6. It is also made from glass-fibre reinforced plastics and contains the installation of the pressure tubing. The spanwise location of the glove is defined at the inner part of the wing by the pro-

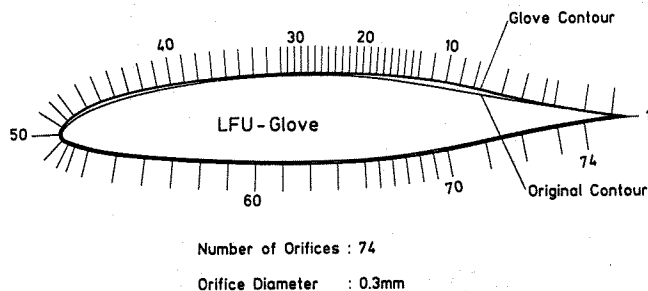


Fig. 5 Comparison of Original and Glove Contour

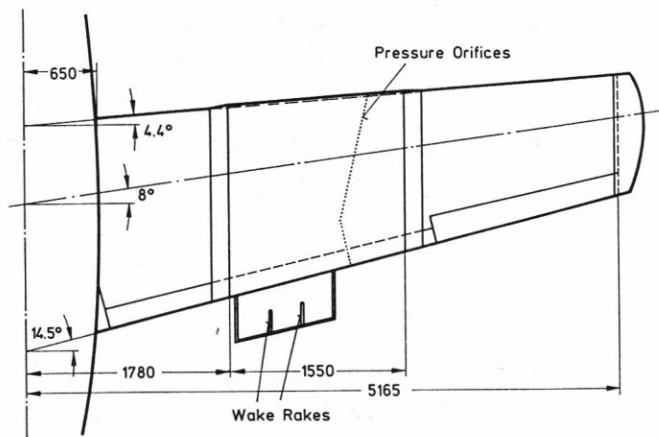


Fig. 6 Laminar Glove on LFU-205 Wing

pellier slip stream not disturbing the glove and at the outer part by the beginning of the aileron. The pressure orifices are arranged on an oblique line compared to the streamwise direction in order to avoid disturbances from orifices lying in front of others. Furthermore the glove is equipped with a wake rake outside the spanwise location of the pressure orifices.

The transition location is determined by means of the infrared technique which is described in details in [11]. The infrared camera is installed inside the cabin of the LFU-205 as shown in Fig. 7 looking to the upper surface of the glove. The advantage of this transition detection technique is the capability of inspecting the complete glove surface. Thus the information of transition of the whole area is available and not only at one point, as provided by some other methods (e.g. hot films).

Flight data and pressure data are acquired by a flight measurement system based on a small computer. The pressure data can be inspected in flight by a quick look system. All data are stored on a data cassette and will be evaluated on ground.

#### 4. Flight tests

Fig. 8 shows the LFU-205 equipped with the glove on the right wing during the first test flights. Significant changes in flight mechanics behaviour, especially in stall behaviour, could not be observed.

Aerodynamic flight test were carried out in a speed range from 80 to 180 kts, in flight levels between 4000 and 10000 ft and with different flap deflections, resulting in chord length Reynolds numbers of 3 to 10 millions. In order to avoid turbulence by thermal convection all measurements took place in flight levels above a temperature inversion. A typical flight test result will be demonstrated in the next figures.

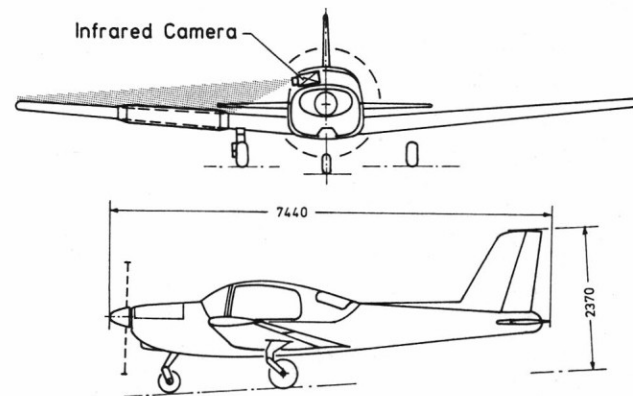
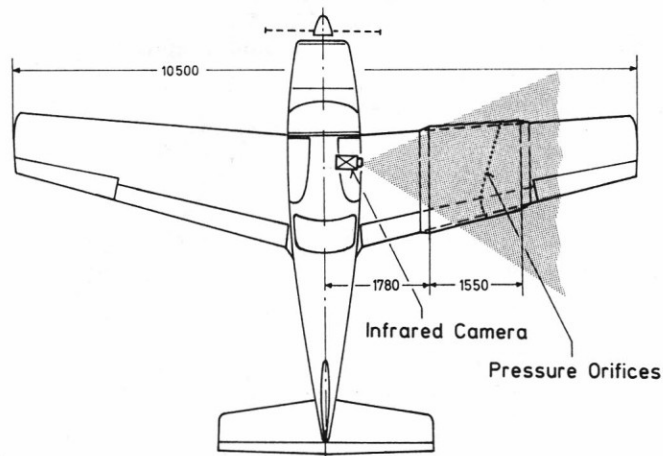


Fig. 7 Installation of Infrared Camera on LFU-205

An infrared image of the upper side of the right wing with the glove at  $Re = 9.5 \cdot 10^6$  is shown in Fig. 9. The light colour in the front part of the glove indicates laminar boundary layer, whereas the dark colour at the rear part of the wing is representative for the turbulent boundary layer. Transition occurs at 47% of the chord length and can easily be detected by the distinct change in colour.

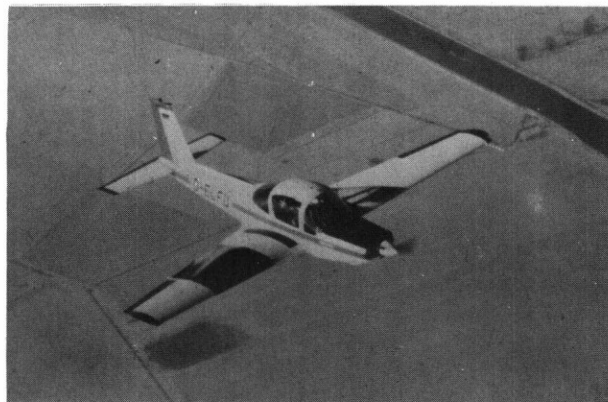


Fig. 8 LFU-205 Aircraft with Laminar Glove in Flight

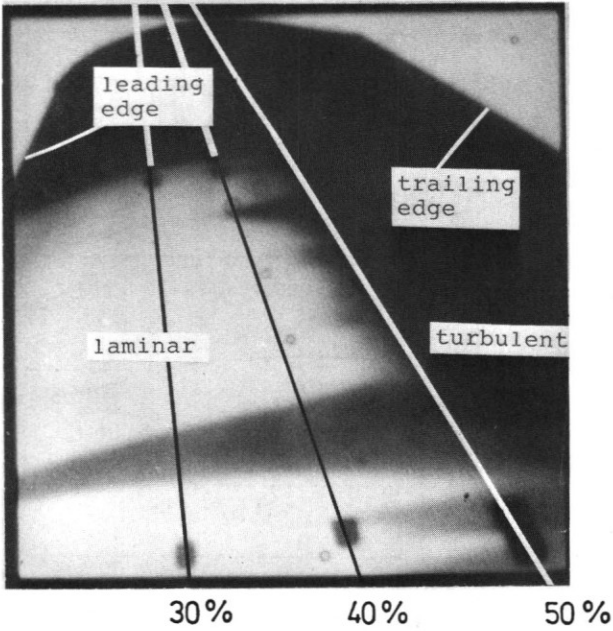


Fig. 9 Infrared Image of LFU-205 Glove in Flight

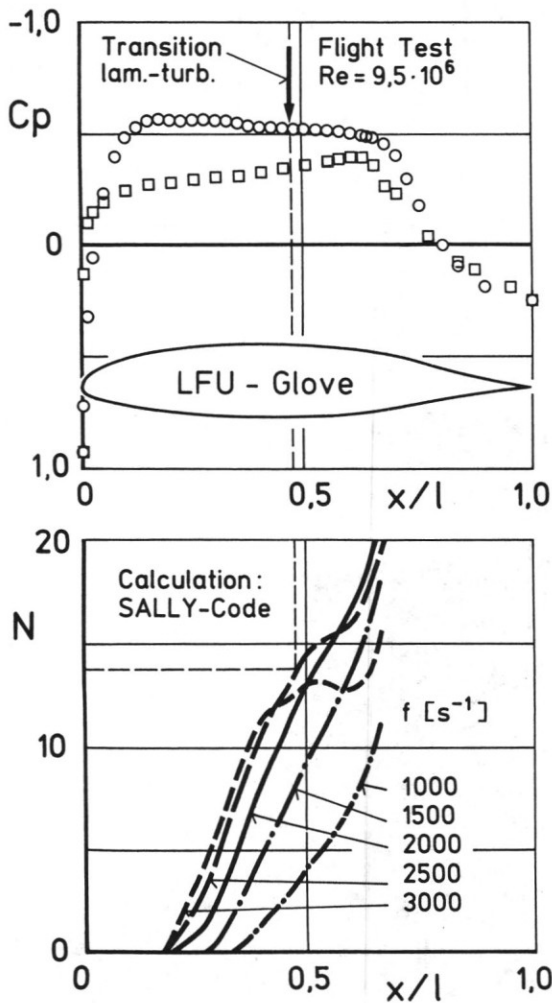


Fig. 10 Flight Test Pressure Distribution and Growth of N-Factor of TS-Waves on LFU-205 Glove

The turbulent wedge in the foreground is induced by an artificial roughness.

The corresponding upper side pressure distribution is shown in the upper part of Fig. 10, marked by the circles. It is the typical design pressure distribution of the glove described in chapter 3. The transition location, found by means of the infrared system, is indicated by an arrow. The scattering in the measured pressure is so low that the small pressure jump induced by the transition process can clearly be seen in the original plots.

The results of the boundary layer stability analysis of the measured pressure distribution by means of the SALLY-code is given in the lower part of Fig. 10. Amplification factors  $N$  selected out of all frequencies investigated are shown versus the chordwise position. At the transition location the envelope leads to a limiting  $N$ -value of  $N \approx 13.5$ .

### 5. Windtunnel tests

Although flight tests are very close to reality experiments in the German-Dutch Windtunnel (DNW) with the LFU-205 wing have been carried out. Windtunnel tests are often cheaper than flight tests and certain experiments can only be done there. The main objective of the windtunnel tests was the determination of a correlation between transition in free flight and DNW; thus qualifying DNW for laminar flow investigations. It should be noted here, that the DNW transition data cannot be transferred to other windtunnels, due to differences in flow quality. The right



Fig. 11 LFU-205 Wing in the 6x8 m<sup>2</sup> Test Section of DNW

wing of the LFU-205 was installed into the 6x8 m<sup>2</sup> closed test section as demonstrated in Fig. 11. The wing was erected vertically in the test section on a steel spike which fits into the wing spar. Due to restrictions in wing strength only parts of the glove section polars could be measured (e.g. max. lift at max. speed will overstress the wing). The same measurements as in flight were carried out.

Fig. 12 gives the pressure distribution, transition location and calculated N-factors for the high speed case at the maximum Reynolds number of  $Re = 9.5 \cdot 10^6$ . Transition, detected by an infrared image, takes place at  $x/l = 0.40$  and is marked by an arrow.

The stability analysis of the measured pressure distribution is shown by the N-factor development at selected frequencies along the wing chord. At the transition location  $x/l = 0.4$  a maximum value of  $N = 13$  is achieved in a frequency range of  $f = 3000$  Hz. Higher values of  $f$ , not shown here, will result in lower N-factors. Thus the limiting N-value is  $N = 13$ .

The comparison of the pressure distribution measured in DNW (Fig. 12) and in free flight (Fig. 9) shows, although the same flow conditions existed, some remarkable differences. In the windtunnel the transition location is shifted forward to  $x/l = 0.40$  and the pressure distribution shows a small depression in that region.

This is due to a different deformation of the wing in the windtunnel compared to free flight caused by a higher dynamic pressure in the windtunnel at the same Reynolds number (temperature effect) and by the different wing attachment in wind-tunnel and free flight.

But this effect does not have any consequences on the data evaluation, because differences in pressure distribution will be considered in the stability analysis of the corresponding laminar boundary layer.

The procedure described above has been applied to several data points with various pressure distributions obtained at different angles of attack, Reynolds numbers and flap positions.

Fig. 13 shows the corresponding infrared image of the wing glove. The flow is from left to right and the laminar boundary layer is indicated by the dark region whereas turbulent boundary layer is marked white. A transition line is clearly visible at 40% of the wing chord. The effect of the pressure holes on the transition location in the upper part of the photo can be detected where a small forward shift of the transition line is visible.

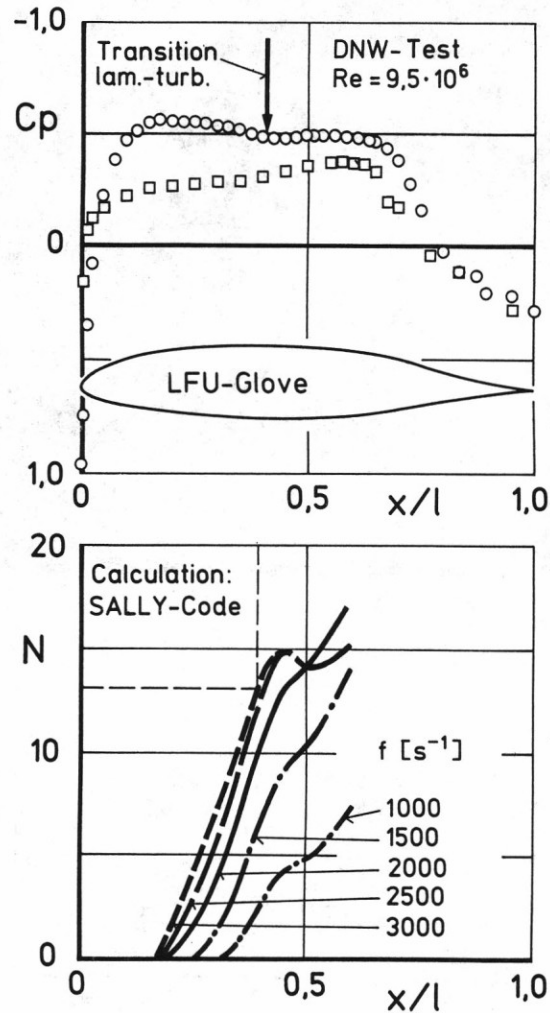


Fig. 12 DNV Test Pressure Distribution and Growth of N-Factor of TS-Waves on LFU-205 Glove

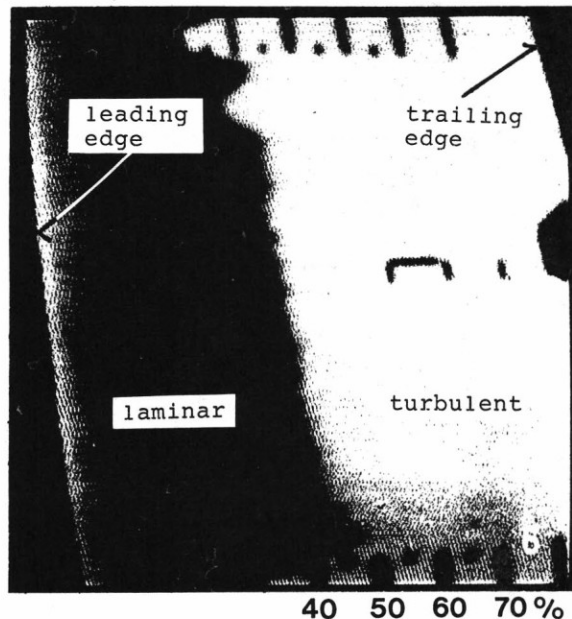


Fig. 13 Infrared Image of LFU-205 Glove in DNW

## 6. Correlation between flight and windtunnel tests

In Fig. 14 the limiting N-values of various data points have been collected and are plotted against the Reynolds number  $Re_T$  based on the length of the laminar boundary layer.  $Re_T$  is varying from  $1 \cdot 10^6$  to  $7 \cdot 10^6$ . Each data point has a different pressure distribution which at the lowest Reynolds number shows a distribution with an adverse pressure gradient at high lift coefficient whereas at the highest Reynolds number pressure distributions with zero pressure gradient have been investigated.

Two sets of data are indicated in Fig. 14: data from flight tests and data from DNW tests, where each set of data contains points at two different flap settings. Two remarkable points should be noted here:

- The limiting N-values are nearly independent of the Reynolds number and of the pressure distribution, although a slight decrease with Reynolds number can be stated. The limiting N-values of TS-waves are  $N \approx 13.5$ .
- There is only a small difference between windtunnel and flight tests in the limiting N-values.

The values of  $N \approx 13.5$  are rather low values for free flight tests. It is imaginable that the presence of engine and propeller noise and structural vibrations may influence the transition behaviour. First flight tests, however, showed that the propeller RPM seems to have no visible effect on transition. Further flight tests with engine off, to be performed in the near future, will help to clarify the situation.

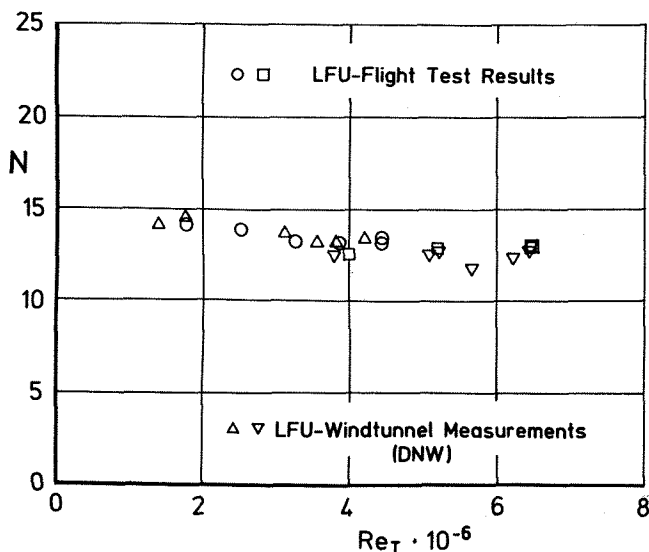


Fig. 14 Calculated N-Factors of TS-Waves at Transition based on Flight and Windtunnel Tests (O  $\Delta$  0° Flap;  $\square$   $\nabla$  3.5° Flap)

The values of  $N \approx 13.5$  for the DNW data indicate the excellent flow quality of this windtunnel test section, because only transition conditions corresponding to values of  $N \approx 12$  for low turbulence wind-tunnels have been stated in the past, e.g. [12].

With the knowledge of the relationship between N-values from flight tests and DNW tests a good correlation concerning the transition behaviour is established.

## 7. Conclusions

Flight and windtunnel investigations concerning boundary layer transition have been performed with the four-seat aircraft LFU-205 of DFVLR. With carefully planned and executed experiments and a following stability analysis of the laminar boundary layer, limiting N-values of Tollmien-Schlichting waves in free flight and in the  $6 \times 8 \text{ m}^2$  test section of DNW have been evaluated. These values will serve as input for a transition prediction with the  $e^N$  or N-factor method. The experiments were performed on a wing glove especially designed for this purpose and comprised pressure measurements and transition location detection by means of infrared images.

From these investigations the following conclusions can be drawn:

- The N-values are nearly independent from the type of pressure distribution and from the transition Reynolds number  $Re_T$  in the range  $1 \cdot 10^6 < Re_T < 7 \cdot 10^6$ .
- Limiting N-values of Tollmien-Schlichting waves in free flight of  $N \approx 13.5$  have been evaluated.
- Limiting N-values of Tollmien-Schlichting waves in the  $6 \times 8 \text{ m}^2$  test section of DNW of  $N \approx 13.5$  have been evaluated.
- These N-values are in the same order of magnitude as the values for free flight, demonstrating the excellent flow quality of DNW.
- The detection of the transition location by means of infrared images proved to be simple, reliable and area covering.

Further flight and windtunnel tests concerning boundary layer measurements with hot wires are under preparation in order to measure frequencies, wave lengths and amplitudes of amplified Tollmien-Schlichting waves.

### References

- [1] Granville, P.S.: The calculation of the viscous drag of bodies of revolution. David Taylor Model Basin Report 849, 1953.
- [2] Michel, R.: Critère de transition et amplification des ondes d'instabilité laminaire. La Recherche Aérosp. No. 70, 1979.
- [3] Jaffe, N.A.; Okamura, T.T.; Smith, A.M.O.: Determination of spatial amplification factors and their application to predicting transition. AIAA Journ., Vol. 8, 1970, pp. 301-308.
- [4] Runyan, J.; George-Falvy, D.: Amplification factors at transition on an unswept wing in free flight and on a swept wing in windtunnel. AIAA-paper No. 79-0267, 1979.
- [5] Hefner, J.N., Bushnell, D.M.: Status of the linear boundary layer stability theory and the  $e^N$  method with emphasis on swept-wing applications. NASA TP-1645, 1980.
- [6] Obara, C.J.; Holmes, B.J.: Flight-measured laminar boundary layer transition phenomena including stability theory analysis. NASA TP 2417, 1985.
- [7] Schlichting, H.: Boundary layer theory. 7. Ed. Mc Graw-Hill, New York, 1979.
- [8] Redeker, G.; Horstmann, K.H.: Die Stabilitätsanalyse als Hilfsmittel beim Entwurf von Laminarprofilen. DFVLR-IB, 1986.
- [9] Eppler, R.; Somers, D.M.: A computer program for the design and analysis of low-speed airfoils. NASA TM 80210, 1980.
- [10] Skrokowski, A.J.; Orszag, S.A.: SALLY level II user's guide. COSMIC Program No. LAR-12556, 1979.
- [11] Quast, A.: Detection of transition by infrared image technique. ICIASF'87 Record, 1987, pp. 125-133.
- [12] Braslow, A.L.; Visconti, F.: Investigation of boundary-layer Reynolds number for transition on an NACA 65(215)-114 airfoil in the Langley twodimensional low-turbulence pressure tunnel. NACA TN 1704, 1948.